Macromolecules 1984, *17*, 2316–2325

Viscoelastic Properties and Relaxation Mechanisms of Binary Blends of Narrow Molecular Weight Distribution Polystyrenes

Hiroshi Watanabe and Tadao Kotaka*

Department of Macromolecular Science, Faculty of Science, Osaka University, Toyonaka, Osaka 560, Japan. *Received November 30, 1983*

ABSTRACT: Viscoelastic properties of binary blends of low and high molecular weight polystyrenes (designated as 1-chain and 2-chain, respectively) each having narrow distribution were examined. In the relaxation spectra of the blends with the content w_2 of 2-chain below a certain critical value w_c, a shoulder of Rouse-wedge type appears after the box-type spectrum of 1-chain. Its characteristic time τ_{12} is proportional to $w_2{}^0M_{w1}{}^3M_{w2}{}^2$, where M_{wi} (i = 1, 2) is the weight-average molecular weight of i-chains. In those of the blends with w_2 sufficiently larger than w_c, a boxlike spectrum with the characteristic time τ_{22} appears after this Rouse wedge. The τ_{22} is proportional to $w_2{}^pM_{w1}{}^0M_{w2}{}^{3.5}$ with $1 \le p \le 1.5$. Molecular pictures for these relaxation modes are discussed in terms of the tube model including *reptation*, *contour length fluctuation*, and *tube renewal processes*. The Rouse-wedge-type mode with τ_{12} in the blends with $w_2 < w_c$ is attributable to the relaxation of 2-chains by renewal of the tube composed of 1-chains. The box-type mode in those with $w_2 > w_c$ is attributable to the reptation of 2-chains from their own tubes, although at intermediate times the 2-chains also relax partly by renewal of the tube composed of 1-chains. On the basis of these pictures, a blending law is proposed. The law takes different forms for those with w_2 below or above w_c. The law describes fairly well the behavior of these blends, including their zero-shear viscosity and recoverable compliance over a wide range of w_2.

Introduction

During the last 20 years, the viscoelastic properties of flexible linear polymers have been extensively studied especially on polymers with narrow molecular weight distribution (MWD). As a result of these studies, it has been clearly recognized that polymeric liquids exhibit the entanglement effects on the rheological properties when the molecular weight exceeds a certain characteristic value M_c. We now have a thorough picture on the entanglement effects in these monodisperse polymer systems.[1,2] Experimental data on the molecular weight M and concentration c dependences of some important parameters such as the zero-shear viscosity η_0, and the steady-state compliance $J_e{}^0$, and the rubbery plateau modulus $G_N{}^0$ are summarized as follows:

$$\eta_0 \propto cM, \qquad J_e{}^0 \propto c^{-1}M, \qquad \text{for } M < M_c \tag{1}$$

$$\eta_0 \propto c^aM^b, \qquad J_e{}^0 \simeq (G_N{}^0)^{-1} \propto c^{-a'}M^0, \quad \text{for } M > M_c \tag{2}$$

$$G_N{}^0J_e{}^0 \simeq 3, \qquad \text{for } M > M_c \tag{3}$$

where a (=4.5–5), a' (=2–2.3), and b (=3.4 ± 0.1) are the parameters almost independent of the particular polymer and solvent species involved.[1,2] The characteristic molecular weight M_c somewhat differs for η_0 and for $J_e{}^0$. For concentrated solutions, the M_c for η_0 is given as

$$M_c \simeq \phi_2{}^{-1}M_c{}^0 \tag{4}$$

where $M_c{}^0$ is the value of M_c for the bulk polymer, and ϕ_2 is the volume fraction of the polymer. Applying the theory of rubber elasticity to $G_N{}^0$, we can define the average molecular weight M_e between the entanglement points. The M_e is roughly half of the M_c for η_0.

On the basis of these experimental results, molecular theories accounting the entanglement effects have been developed.[3-10] Williams et al.[10] proposed an extended Rouse model, introducing concepts of elastic coupling and enhanced friction of the Rouse beads representing the entanglement points, and successfully simulated the rheological behavior of flexible polymers.

On the other hand, de Gennes[5,6] and Doi and Edwards[7-9] proposed the "tube model" theory, in which the entanglement effect is regarded as due to the topological constraint imposed on a given chain by surrounding chains acting as spatially fixed obstacles. The chain can move by curvilinear diffusion along its contour as if it is confined in a tube. Such a motion was called *reptation*.[5-9] There still remain some discrepancies between the tube theory and experimental results on η_0, $J_e{}^0$, and $G_N{}^0J_e{}^0$. However, they have been accounted for by introducing some additional concepts such as constraint release by *tube renewal*[11,12] and *contour length fluctuation* of the reptating chain.[12,13]

The viscoelastic properties of flexible polymers having broad MWD have also been a subject of extensive studies[1,2,14-22] to elucidate the effects of polydispersity. In such studies, binary blends of narrow MWD polymers were the simplest model system, for which several characteristic features were found. When the molecular weights of the component polymers do not differ much, the terminal zone of the viscoelastic functions such as the relaxation spectrum becomes broader. On the other hand, when the molecular weights are quite different, a two-step rubbery plateau appears.

Some phenomenological blending laws were proposed for predicting the dependence of η_0 and $J_e{}^0$ on molecular weights and blending ratio for such binary blends.[4,14,16-19] However, there are still only a few attempts[20,22] carried out for accounting the polydispersity effects on a molecular basis. Since the tube model had been successful in describing the rheological as well as self-diffusion behavior of monodisperse polymers in a simple and clear manner, we were tempted to extend this concept to explain the behavior of binary blends and to construct a blending law on the basis of the tube model.[23-25] Conceivably there are various different relaxation processes involved in such blends or polydisperse polymers. To clarify and separate the different relaxation processes, we prepared a series of binary blends composed of monodisperse polymers having widely different molecular weight and with varying blending ratio. Then we studied their linear viscoelastic properties. In this paper, we present the results and discuss possible relaxation mechanisms in the blends on the basis of the tube model which includes the concepts of *reptation*, *contour length fluctuation*, and constraint release by *tube renewal*.

Experimental Section

Anionically polymerized narrow MWD polystyrene (PS) samples were used in this study. The characterization of the samples was carried out on a gel permeation chromatograph (GPC; Toyo

0024-9297/84/2217-2316$01.50/0

Table I
Characteristics of Polystyrene Samples

code	$10^{-3}M_n$	M_w/M_n
L22	21.8	1.07
L36	36.3	1.07
L68	68.3	1.06
L407[a]	407	1.05
L1070	1070	1.11
L2580[a]	2580	1.09

[a] Supplied from Toyo Soda Mfg. Co. Ltd.

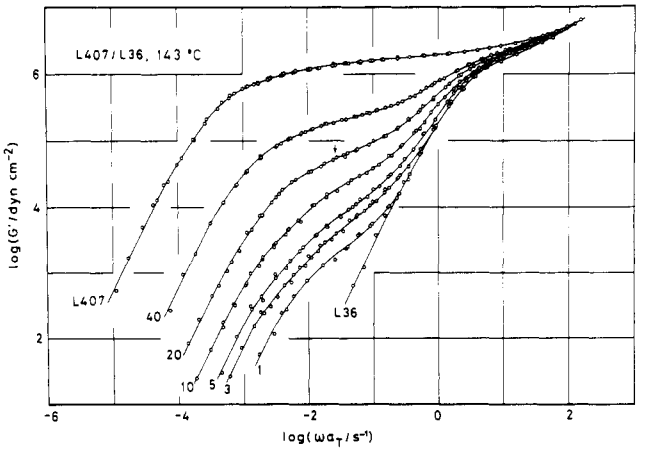

Figure 1. Master curves of the storage moduli G' for L407/L36 blends reduced at 143 °C. The numerical values represent the content w_2 in wt % of L407 in the blends.

Soda, Ltd., Model HLC-801A) equipped with a triple-detector system consisting of a built-in refractometer, a UV monitor (Toyo Soda, Ltd., Model UV-8), and a low-angle laser-light scattering photometer (Toyo Soda, Ltd., LS-8). Chloroform was the elution solvent, and commercially available PS elution standards (Toyo Soda, Ltd., TSK PS samples) were used. Table I shows the characteristics of the samples.

To prepare binary blends, we chose two PS samples with the molecular weight differing at least by 1 order of magnitude. The two samples were dissolved in benzene to make a 5 wt % solution. Then the solution was freeze-dried for 12 h and further dried at 80 °C under vacuum for 24 h. The dried blend was then molded at about 170 °C by a laboratory hot press into disks of about 26-mm diameter and 1.3-mm thickness. For reference, component PS samples were also tested. However, the two high molecular weight samples, L1070 and L2580, were too rubbery to be molded into disks. Therefore, we did not test these samples.

Dynamic measurements were carried out at several temperatures between 127 and 236 °C with a conventional cone-and-plate rheometer (Autoviscometer L-III, Iwamoto Seisakusho, Kyoto). The radius of the cone was 15.0 mm, and the angle between the cone and plate was 3.68°. The storage G' and loss G''*moduli* were determined by the Markovitz equation,[26] and the time–temperature superposition principle[1] was applicable.

For convenience, we designate the low molecular weight component as "1-chain" and the high molecular weight one as "2-chain". Hereafter, the subscripts 1 and 2 refer to the quantities of the 1- and 2-chains, respectively.

Results and Discussion

Master Curves and Relaxation Spectra. Figures 1 and 2, respectively, show the master curves of G' and G'' reduced at 143 °C for L407/L36 blends. The numerical values in the figures represent the content w_2 in wt % of the 2-chain (L407 in this case). Both of the 1- and 2-chains have a molecular weight larger than the so-called molecular weight between entanglement points M_e^0 (= 18 × 10^3)[1,2] for monodisperse bulk polystyrenes. They exhibit a rubbery plateau in the G' and G'' curves.

In the G' and G'' curves for the blends a shoulder appears, although the one in the G'' curve is less prominent.

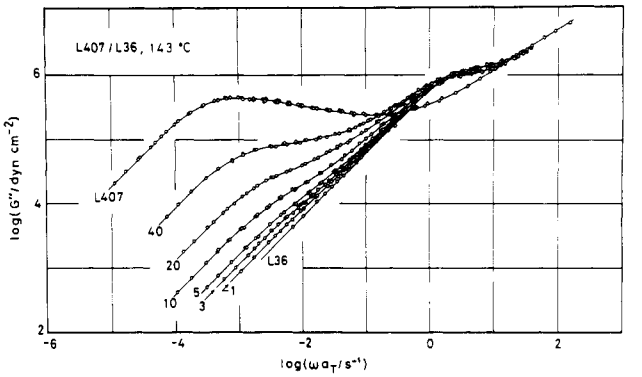

Figure 2. Master curves of the loss moduli G'' for L407/L36 blends reduced at 143 °C. The numerical values represent the content w_2 in wt % of L407 in the blends.

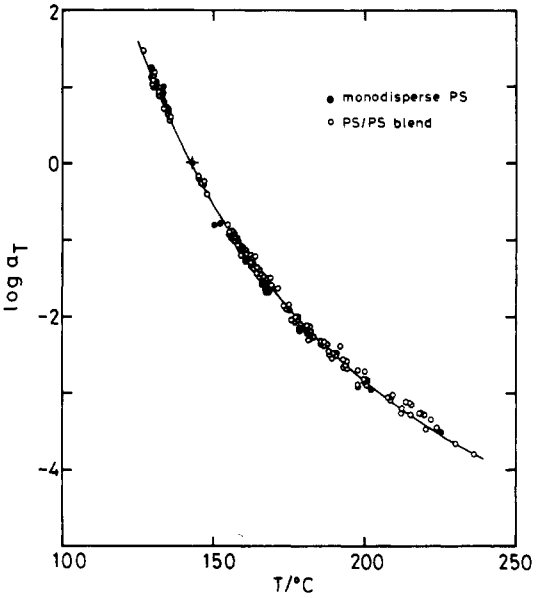

Figure 3. Temperature dependence of the shift factor a_T of the binary blends and monodisperse polystyrenes. The solid curve represents the WLF equation with the reference temperature T_r = 143 °C.

Their position is independent of w_2, but the height increases with increasing w_2 until w_2 reaches 5 wt %.

When w_2 exceeds 5 wt %, the shoulder becomes a plateau, and the plateau extends to the low-frequency side with further increase in w_2. A similar two-step rubbery plateau was already reported by various authors[15-22] for blends having large w_2. However, examining carefully the lower plateau, we notice that this plateau is not flat but has a small inflection (marked by the arrow on the G' curve of 20 wt % blend). The location of this inflection roughly corresponds to that of the shoulder for the blends with w_2 less than 5 wt %. Similar results were obtained also for other blends.

Figure 3 shows the temperature dependence of the shift factor a_T for all the blends and constituent PS samples examined here. The solid curve in the figure represents the WLF equation[1] with the reference temperature T_r = 143 °C. All the systems exhibit the same a_T vs. temperature relation within experimental errors.

Figures 4–6 show the relaxation spectra H of the blends determined by the second-order Tschoegl approximation[27] from the G' and G'' curves reduced at 143 °C. For 20 wt % L407/L36 and L1070/L36 blends, the H calculated from the G' (represented by circles) and G'' (triangles) curves are shown. They coincide with each other within the accuracy of the Tschoegl approximation.

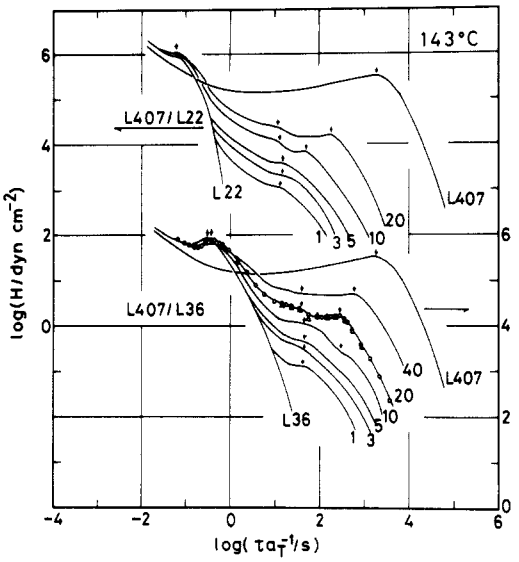

Figure 4. Relaxation spectra of L407 blends reduced at 143 °C. The numerical values represent the content w_2 in wt % of L407 in the blends.

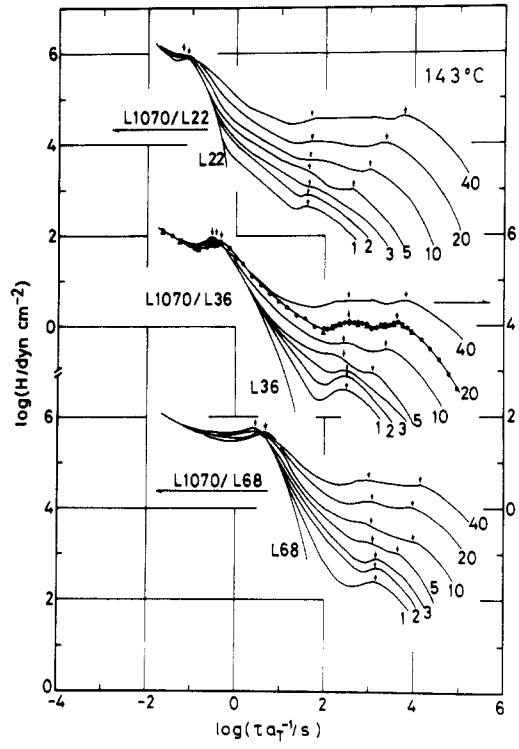

Figure 5. Relaxation spectra of L1070 blends reduced at 143 °C. The numerical values represent the content w_2 in wt % of L1070 in the blends.

In these figures, we notice the following features. All the monodisperse PS samples exhibit box-type spectra. For the blends, there is a critical content w_c of the 2-chain: when w_2 is less than their w_c, a box-type spectrum corresponding to that of the 1-chain appears, and then a wedgelike shoulder follows. The position of the shoulder remains independent of w_2, but its height increases as the w_2 is increased to w_c. When w_2 exceeds w_c, the wedgelike end of the spectrum becomes boxlike, and its end extends to the longer time side with further increase in w_2. However, a small maximum (came from the inflection of the master curves) still remains in the H at almost the same position as that of the shoulder for the blends with w_2 below w_c. This small maximum becomes less significant as w_2 is further increased. Since both G' and G'' curves

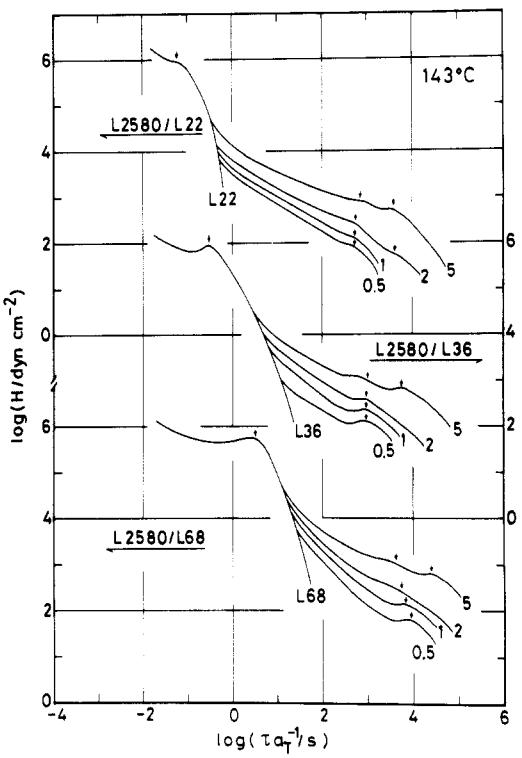

Figure 6. Relaxation spectra of L2580 blends reduced at 143 °C. The numerical values represent the content w_2 in wt % of L2580 in the blends.

Table II
Comparison of the Molecular Weight M_{w2} of the 2-Chain (the High Molecular Weight Component) and Characteristic Molecular Weight M_c at Its Critical Content w_c

blend	w_c/wt %	$10^{-3}M_{w2}$	$10^{-3}M_c$[a]
L407/L22	5–10	422	360–720
L407/L36	5–10	422	360–720
L1070/L22	3–5	1190	720–1200
L1070/L36	3–5	1190	720–1200
L1070/L68	3–5	1190	720–1200
L2580/L22	1–2	2810	1800–3600
L2580/L36	1–2	2810	1800–3600
L2580/L68	1–2	2810	1800–3600

[a] Estimated by eq 4; $M_c^0 = 36 \times 10^3$.

give an identical spectrum, this small maximum seems not to be an artifact.

From the H shown in Figures 4–6, we determined the critical content w_c for each blend, above which the boxlike spectrum emerges at long times. The results are summarized in Table II. The w_c is dependent on the weight-average molecular weight M_{w2} of the 2-chain but not on the M_{w1} of the 1-chain. We estimated the characteristic molecular weight M_c for solutions of the 2-chain with the content w_c in the 1-chain by eq 4, assuming that the partial specific volumes of the 1- and 2-chains are equal in the blend and, hence, ϕ_2 is equal to w_2. The values of M_c are compared with M_{w2}. Although the estimation of M_c by eq 4 for such semidilute solutions with w_c below 10 wt % is somewhat ambiguous, the values of M_{w2} are found in the range of M_c estimated. Thus, the w_c seems to correspond to the onset of the entanglements among the 2-chains.

The binary blends examined here exhibit at least three different relaxation modes: the relaxation of 1-chains entangled with other 1- and/or 2-chains represented by the box-type spectrum at short times, the relaxation of

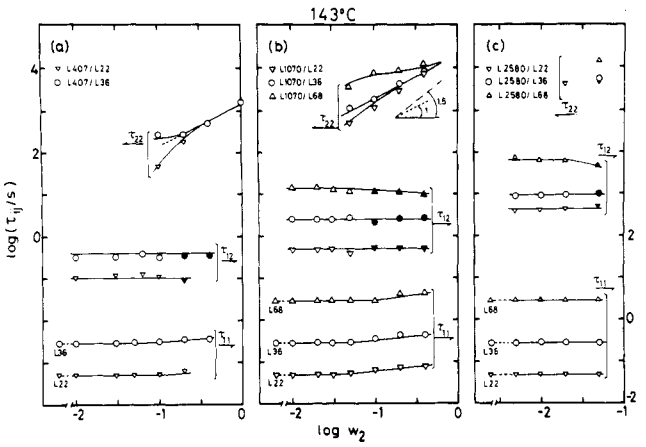

Figure 7. Dependence of the characteristic times τ_{ij} of the binary blends at 143 °C on the content w_2 of the 2-chains. The filled symbols represent the values of τ_{12} obtained by dividing the relaxation spectra according to the blending law eq 13.

2-chains from the entanglements with 1-chains, resulting in the wedgelike shoulder or the small maximum at intermediate times, and the relaxation of 2-chains from the entanglements among themselves represented by the box-type spectrum at long times. Obviously, the last mode would not appear when w_2 is below w_c, because at these low concentrations the 2-chains no longer overlap among themselves enough to entangle with one another.

Characteristic Relaxation Time. We estimated the characteristic relaxation times τ_{ij} from the positions of the peaks in the boxlike and/or the wedgelike portions of the spectra as indicated by the arrows in Figures 4–6. We designated these characteristic times as τ_{11}, τ_{12}, and τ_{22} from the short-time side. Figure 7 shows plots of these τ_{ij} vs. w_2.

Since the maxima in the H at intermediate times are small and broad for the blends with w_2 above w_c, it was not easy to estimate τ_{12} directly from the H shown in Figures 4–6. For such blends, we split the spectrum into four portions by employing the blending law that will be discussed later and estimated the τ_{12} from the corresponding portion of the spectrum. These results are shown by filled marks in Figure 7. The τ_{12} for the blend with $w_2 > w_c$ estimated this way roughly coincides with the position of the small and broad maximum in H, as shown in Figures 4–6.

The dependences of τ_{ij} on w_2 and molecular weights are summarized as follows. The τ_{11} is almost independent of w_2 and coincides with the characteristic relaxation time τ_1 for the component 1-chain. With increasing w_2, the τ_{11} increases a little. The τ_{12} is almost independent of w_2 over the full range of w_2 examined. Although τ_{12} might decrease slightly with increasing w_2 at large w_2, the change of τ_{12} is so small that we cannot judge whether τ_{12} decreases or remains constant. Figure 8 summarizes the M_{w1} and M_{w2} dependences of τ_{12}. On the other hand, the τ_{22} exhibits a contrasting difference from the τ_{11} and τ_{12}. For the blends with w_2 below w_c, the τ_{22} cannot be defined. For those with w_2 sufficiently larger than w_c (w_2 = 20 and 40 wt %), the τ_{22} becomes independent of M_{w1} but becomes proportional to the 3.5th power of M_{w2}. These results may be cast into the following power law forms:

$$\tau_{12} \propto w_2^0 M_{w1}^3 M_{w2}^2 \quad (5)$$

$$\tau_{22} \propto w_2^p M_{w1}^0 M_{w2}^{3.5} \quad (w_2 > w_c \text{ and } \tau_{22} \gg \tau_{12}) \quad (6)$$

where the exponent p ranges from 1 to 1.5.

Intensity of Relaxation Modes. We estimated the intensities P_{ij} of each of the modes ij from the heights at

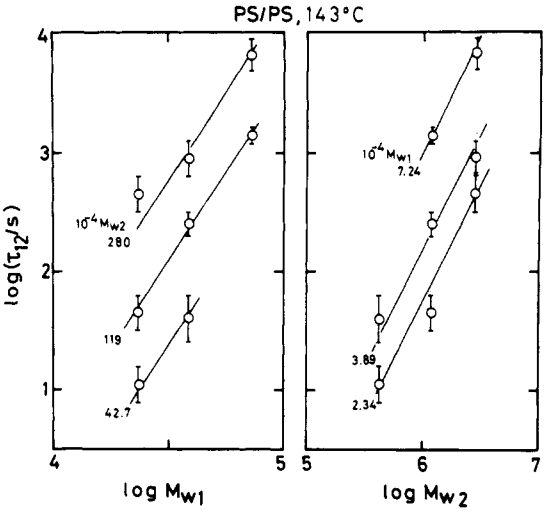

Figure 8. Dependences of τ_{12} of the binary blends at 143 °C on the molecular weights M_{w1} and M_{w2} of the 1- and 2-chains, respectively. Note that the scale of the horizontal axis is different in the left and right panels.

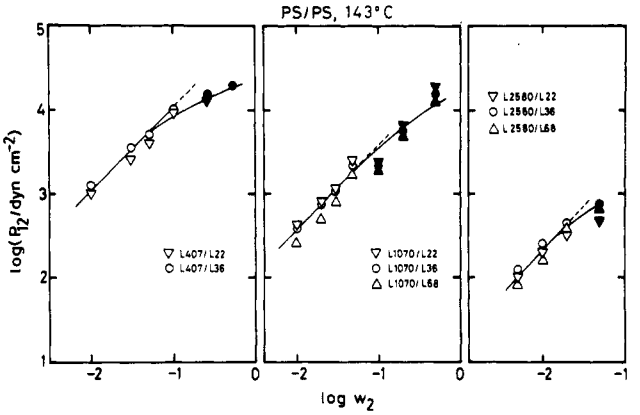

Figure 9. w_2 dependence of the intensity P_{12} of the wedge-type relaxation spectra at intermediate times for the binary blends. The filled symbols were the values obtained by dividing the relaxation spectra according to the blending law eq 13.

τ_{ij} of the spectra. Figure 9 shows the w_2 dependence of P_{12}. The filled symbols again represent the values estimated by applying the blending law. On the other hand, Figure 10 shows the plot of P_{22} vs. w_2.

The P_{12} is proportional to w_2 at small w_2 but seems to deviate downward from the proportionality at large w_2, as seen in Figure 9. In addition, the P_{12} at small w_2 is almost independent of M_{w1} but is inversely proportional to M_{w2}. This behavior resembles that of Rouse chains.[1,2] In this connection, we should note that the dependence of τ_{12} on M_{w2} in eq 5 also coincides with that of the Rouse chain, and the wedgelike shoulder in the H for the blends with w_2 less than w_c looks like a Rouse wedge.

The P_{22} is proportional to w_2^2 but independent of both M_{w1} and M_{w2}. This result again suggests that the relaxation mode with the longest characteristic time τ_{22} is related to the entanglements among the 2-chains.

Molecular Picture for Relaxation Processes. The tube model[5-9] describes the entanglement effects as follows. An arbitrary chain chosen is called a *test* chain, and other chains entangling with it are regarded as *spatially fixed* obstacles exerting topological constraints on the test chain. Such entangling chains are replaced by a *tube* or a series of *slip-links* for the test chain. According to the original Doi–Edwards theory,[7] the slow mechanical relaxation in such a system takes place when the test chain escapes from the tube by its reptation, while the tube does not change

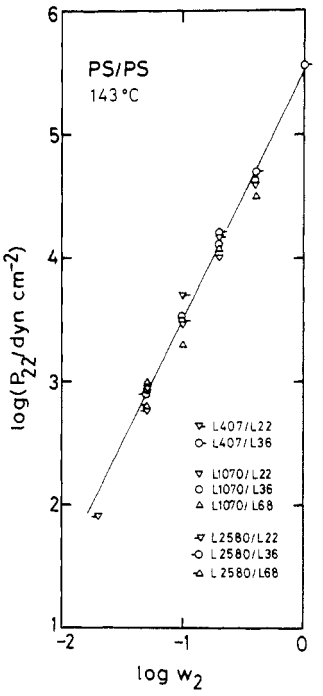

Figure 10. w_2 dependence of the intensity P_{22} of the box-type relaxation spectra at long times for the binary blends.

its spatial orientation and shape. This process may be called *pure reptation*. The Doi–Edwards theory assumes that the contour length of the reptating chain is unconstrained and always assumes its equilibrium length, but its spatial orientation is constrained by the tube. Thus the pure reptation is the only relaxation mode appearing in the time scale slower than the intrachain Rouse modes.

Recent theoretical works[11-13] suggested that the above assumptions are justifiable only if the polymer chain has the molecular weight sufficiently larger than M_e. On the other hand, if it is not much larger than M_e, some other relaxation modes become significant. One is constraint release by *tube renewal*, in which the tube itself disengages by the reptation of the chains forming the tube. Then the constraint imposed on the test chain would be released by Rouse relaxation modes.[11,12] The other is *contour length fluctuation* of the test chain,[12,13] becoming significant when the fluctuation is no longer negligible as compared with the tube length.

We apply these molecular pictures to interpret the relaxation mechanisms in our binary blends. Since all the blends exhibited the same temperature dependence of a_T (cf. Figure 3), and since the G' and G'' curves at high frequency become independent of w_2 (cf. Figures 1 and 2), the first parameter of the tube model, the monomeric friction coefficient ζ_0, is assumed to be the same for any of the components in the blends. Then the second parameter, the number of the monomer units N_e between the entanglement points, plays a key role.

As discussed above, the 1-chains in the blend relax dominantly by reptation. The tube renewal process becomes more and more delayed with increasing molecular weight of the tube-forming chains.[11,12] For a 1-chain in the blend, the confinement due to the 2-chains should persist longer than that due to other 1-chains in the blend or than that on a 1-chain in its bulk. As seen in Figure 7, the τ_{11} is essentially equivalent to the τ_1 of the bulk 1-chain but becomes slightly longer with increasing w_2, reflecting the above situation.

On the other hand, the relaxation modes of a 2-chain in the blend involve those due to two different types of

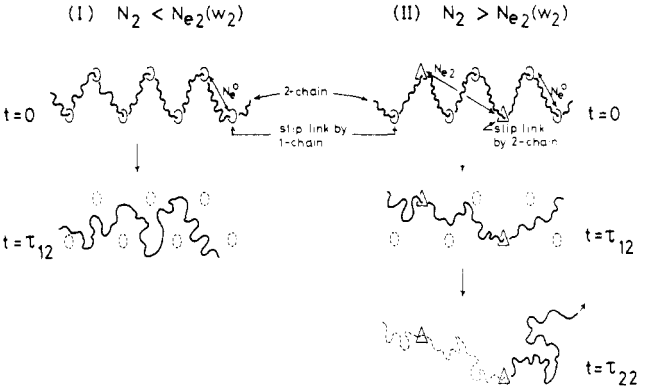

Figure 11. Schematic representation of the molecular mechanisms of the relaxations of the 2-chain in the dilute (I) and concentrated (II) binary blends.

slip-links confining the 2-chain. The first type is due to the 1-chains (type-1 slip-links) and the second type due to the 2-chains (type-2 slip-links). Intuitively, we may say that the type-1 slip-links disappear much faster than the type-2 slip-links.

We can evaluate the number of the monomer units $N_{e2}(w_2)$ between the entanglement points of the second type, assuming that the 1-chains are acting simply as diluent to the 2-chains. Although the total number of the slip-links for a 2-chain remains the same, and hence, the number of the monomer units N_e between all kinds of slip-links is the same as that in the bulk 2-chain, the $N_{e2}(w_2)$ increases with decreasing w_2, and finally at $w_2 \simeq w_c$ it would exceed N_2. In other words, the 2-chains no longer entangle with one another but entangle only with the 1-chains in such a *dilute* blend. Thus we may classify the blends into the following two types, as illustrated in Figure 11, according to the relaxation modes of the 2-chains involved.

(I) Dilute Blends with $w_2 < w_c$ and $N_2 < N_{e2}(w_2)$. In dilute blends, the relaxation modes of the 2-chain are due to the competition of the reptation of the 2-chain to escape from the type-1 slip-links and the tube renewal, i.e., the disappearance of the type-1 slip-links. If the degree of polymerization N_1 of the 1-chain is much smaller than that N_2 of the 2-chain, the latter process would dominate the former. Obviously, as long as $N_2 < N_{e2}(w_2)$, the characteristic time τ_{12} for the tube renewal process should be independent of w_2 and the intensity P_{12} should be proportional to w_2. The results shown in Figures 7 and 9 satisfy this assumption.

Klein[11] and Graessley[12] treated the tube renewal process regarding the array of slip-links as a virtual Rouse chain consisting of N_2/N_e virtual Rouse (tube) segments. They estimated its characteristic time as

$$\tau_{\text{tube renewal}} \simeq (N_2/N_e)^2\tau_c \tag{7}$$

where the characteristic time τ_c of the tube segment is given as that of the pure reptation of a 1-chain as

$$\tau_c \propto N_1^3/N_e \tag{8}$$

Assuming that N_e in eq 7 and 8 may be regarded as equivalent to that for the blend, we obtain

$$\tau_{12} \propto (N_1/N_e)^3N_2^2 \tag{9}$$

This equation is in good agreement with the observed relation (eq 5) for the blends with $w_2 < w_c$.[28]

In some sense, this tube renewal process is similar to retarded Rouse relaxation processes in a highly viscous medium.[1] In fact, the slow Rouse modes appear when the

type-1 slip-links become ineffective. However, one should note that the confinement due to the 1-chains is still effective even after its boxlike spectrum vanishes at long times. That is, in the time scale $\tau_{11} < \tau < \tau_{12}$, the 1-chains already have relaxed but still impose confinements on the 2-chain.

(II) Concentrated Blends with $w_2 > w_c$ and $N_2 > N_{e2}(w_2)$. When w_2 is increased and the $N_{e2}(w_2)$ becomes smaller than N_2, a 2-chain is confined by or entangles with both 1- and 2-chains. Again, if N_1 is much smaller than N_2, the type-1 slip-links disappear first with the relaxation time τ_{12}, partly releasing the constraint on the 2-chain. Then, after the time τ_{12}, the blend may be regarded as a solution of 2-chains dispersed in 1-chains. The remaining constraint on the 2-chain is released by its own reptation or by tube renewal, i.e., the disappearance of the remaining type-2 slip-links. Under such a situation, the dominant relaxation mechanism appears to be the reptation with the time scale τ_{22} accompanying some contributions from contour length fluctuation.

Recently, Doi[13] calculated the disengagement or reptation time $\tau_d^{(f)}$ (= τ_{22} for our blends) for a primitive chain with fluctuating contour length as

$$\tau_d^{(f)} \simeq (\zeta_0 b_s^2/kT)(N_2^3/N_e)[1 - 1.47(N_e/N_2)^{0.5}]^2 \qquad (10)$$

where b_s is the step length of the segment. For the blends with $w_2 > w_c$, the $\tau_d^{(f)}$ corresponds to τ_{22}, provided N_e be replaced by $N_{e2}(w_2)$. For such blends, the $N_{e2}(w_2)$ would be proportional to w_2^{-1} as in usual concentrated solutions.[31] Then from eq 10 we have[32]

$$\tau_{22} \propto w_2^{1.4} N_2^{3.4} \qquad (10')$$

This equation coincides with the observed result (eq 6) except for a small difference in the exponent p to w_2. However, the discrepancy due to this difference in p is rather small for the blends with $w_2 \geq 20$ wt %, for which eq 6 holds.

On the other hand, the w_2 dependence of τ_{12} for the blends with $w_2 > w_c$ poses some problems. Following Klein's[11] and Graessley's[12] treatments, we regard only the type-1 slip-links as virtual Rouse segments. Since the number of the monomer units N_{e1} between adjacent type-1 slip-links would be inversely porportional to w_1, the number of such virtual Rouse (tube) segments N_2/N_{e1} would be proportional to w_1. Then, replacing N_2/N_e by N_2/N_{e1} in eq 7, we obtain τ_{12} proportional to w_1^2. However, as seen in Figure 7, the τ_{12} for the blends is almost independent of w_2 and hence of w_1 over the full range of w_2 examined.

The origin of this discrepancy is not clear. Perhaps the assumption introduced above is too naive. In fact, slip-links or a tube are not real but hypothetical entities representing the constraint imposed by entangling chains on the given test chain. We speculatively suppose that we cannot localize and count the slip-links when we discuss the characteristic time for the tube renewal process. Instead, we can take the length of the (primitive) test chain confined by the slip-links into account. If all chains entangling with the 2-chain have the same molecular weight, as is the case of Klein[11] and Graessley,[12] we obtain the same result either by counting the number of slip-links or by taking the length of the test chain trapped in the slip-links into account. However, in the present blends, these estimations give different w_2 dependences of τ_{12}. Since 2-chains entangle not only with 1-chains but also with other 2-chains, the length of the test 2-chain is independent of w_2. This leads to w_2-independent τ_{12}, which almost agrees with the observed results shown in Figure 7. Clearly, further theoretical study is needed to elucidate the relaxation modes by mixed reptation–tube renewal processes.

The intensities P_{12} and P_{22} of the relaxation modes in the concentrated blends with $w_2 > w_c$ are rather easily understood. In such blends, a part of the constraints is released by the tube renewal (of the type-1 slip-links) and the other by the reptation of the 2-chain. As seen in Figure 9, the intensity P_{12} for the former is first proportional to w_2 and then seems to become less sensitive to w_2 with increasing w_2. On the other hand, the P_{22} for the latter becomes proportional to w_2^2 similar to those for ordinary concentrated homopolymer solutions.

Blending Law. Blending laws proposed so far by various authors[4,14,16-19] are mostly phenomenological and may be cast into the following systematic forms:

$$H_B(\tau) = \sum_i P_i H_i(\tau/\lambda_i) \qquad \text{(first-order law)} \qquad (11a)$$

$$H_B(\tau) = \sum_{ij} P_{ij} H_{ij}(\tau/\lambda_{ij}) \qquad \text{(second-order law)} \qquad (11b)$$

$$H_B(\tau) = \sum_{ijk} P_{ijk} H_{ijk}(\tau/\lambda_{ijk}) \qquad \text{(third-order law)} \qquad (11c)$$

where the intensity factor P's are often represented by the weight fraction of the component polymers as $P_i = w_i$ and $P_{ij} = w_i w_j$, and the components of the relaxation spectrum, H_{ii} and H_{iii}, by H_i of the corresponding monodisperse component i. On the other hand, the shift factor λ's and the cross terms, H_{ij} and H_{ijk}, are often determined empirically so that the calculated spectrum $H_B(\tau)$ satisfactorily accounts the observed values of J_e^0 and η^0 of the blends.

Recently, Kurata[24] and Masuda and co-workers[25] proposed new blending laws based on the tube model. However, Kurata did not incorporate the tube renewal process, while Masuda did so in a way somewhat different from what we have done. Our blending law is based on the pictures discussed above. First of all, it should be noted that our law is essentially the first-order one with respect to the weight fraction of the components.

As is well-known,[1,2] in the transition zone ($\tau < \tau^*$) of the spectrum, the relaxation modes are independent either of molecular weight or of its distribution, provided the blend does not contain any solvent which reduces the monomeric friction coefficient ζ_0. Therefore, the spectra of any blends exhibit an equivalent Rouse wedge in this transition zone. The contributions from the two components are additive on the weight basis.

On the other hand, in the rubbery plateau to terminal zone, the shift factor λ's and the intensity factor P's for each component may differ between those in the dilute ($w_2 < w_c$) and concentrated ($w_2 > w_c$) blends, because the entanglements among 2-chains do not exist in the former. Therefore, the blending law should be distinguished between these two cases.

(I) Dilute Blends with $w_2 < w_c$ and $N_2 < N_{e2}(w_2)$. The relaxation modes of the 1-chains in the blends are essentially the same with those in the bulk 1-chain, except that the relaxation time τ_{11} of the 1-chain in such a blend might be slightly longer than the τ_1 of the bulk 1-chain. Thus in the region where $\tau < \tau_{11}$, the 1-chains exhibit a wedge-and-box spectrum H_{11} with the intensity P_{11} proportional to w_1, and we may replace H_{11} by H_1.[33]

On the other hand, the relaxation modes of the 2-chains are a little more complicated. In the region where $\tau < \tau_{11}$ (in the box spectrum H_{11}), a 2-chain does not distinguish the surrounding 1-chains from other 2-chains. Thus, in this region, the 2-chains give a wedge-and-box spectrum H_{12}^b with the intensity proportional to w_2. Similar to the case of H_{11}, the H_{12}^b may be replaced by H_2 of the bulk 2-chain but only in the region $\tau < \tau_{11}$. Beyond this time scale $\tau_{11} < \tau$, the tube renewal process becomes dominant

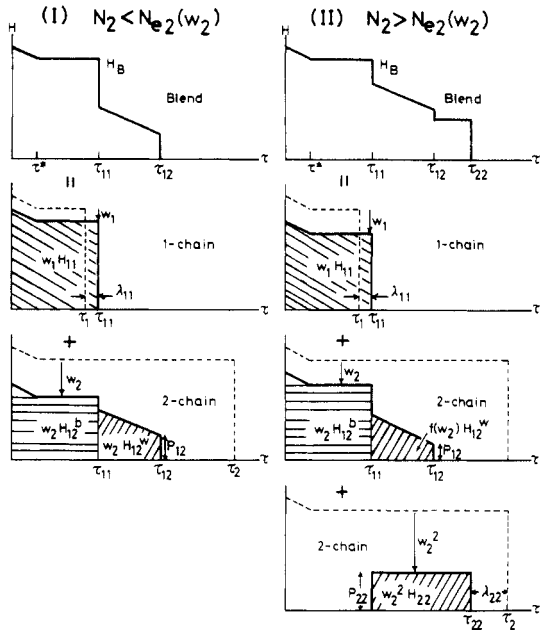

Figure 12. Schematic diagram representing the blending law for (I) the dilute blends in which 2-chains do not entangle with themselves (left) and (II) the concentrated blends in which 2-chains do entangle with themselves (right).

by the diffusion or reptation of the entangling 1-chains. Then, a Rouse-wedge-type spectrum $H_{12}{}^{w}$ with the cut-off time τ_{12} ($\propto M_{w1}{}^{3}M_{w2}{}^{2}$) appears. Its intensity is proportional to $w_2M_{w2}{}^{-1}$ (Rouse mode). These situations are illustrated schematically in the left-hand-side column of Figure 12. Combining these contributions we obtain

$$H_B(\tau) = w_1H_{11}(\tau/\lambda_{11}) + w_2[H_{12}{}^{b}(\tau) + H_{12}{}^{w}(\tau)] \simeq w_1H_1(\tau/\lambda_{11}) + w_2[H_2(\tau)|_{\tau<\tau_{11}} + H_{12}{}^{w}(\tau)] \quad (12)$$

where λ_{11} represents the small difference between τ_{11} and τ_1 and is approximately unity (cf. Figure 7). The first two terms on the right-hand side of eq 12 are zero for $\tau > \tau_{11}$, and only the last term contributes in the range $\tau_{11} < \tau < \tau_{12}$.

(II) Concentrated Blends with $w_2 > w_c$ and $N_2 > N_{e2}(w_2)$. In the blends with $w_2 > w_c$, the relaxation modes of the 1-chains are almost the same as those of the blends with $w_2 < w_c$. The corresponding spectrum may be written as $w_1H_{11}(\tau/\lambda_{11}) \simeq w_1H_1(\tau/\lambda_{11})$ for $\tau < \tau_{11}$. The difference λ_{11} between τ_1 and τ_{11} is somewhat larger than that in the blends with $w_2 < w_c$, corresponding to the shift in τ_{11} with increasing w_2 (cf. Figure 7).

In the region $\tau < \tau_{11}$, the relaxation modes of the 2-chains also are almost the same as those in the blends with $w_2 < w_c$. The spectrum may be written as $w_2H_{12}{}^{b} \simeq w_2H_2(\tau)$ for $\tau < \tau_{11}$. However, in the region $\tau > \tau_{11}$, the 2-chains relax partly by tube renewal of the type-1 slip-links and the rest by their own reptation. The tube renewal process results in a Rouse-wedge-type spectrum $H_{12}{}^{w}$ with the cut-off at τ_{12}. However, uinlike that in the dilute blends, its intensity P_{12} is not proportional to w_2 but is a slightly weaker function $f(w_2)$. Thus, this contribution to the spectrum may be written as $f(w_2)H_{12}{}^{w}$ for $\tau_{11} < \tau < \tau_{12}$. A possible form of $f(w_2)$ might be w_2w_1.

At sufficiently long times $\tau \gg \tau_{12}$, the blend may be regarded as a concentrated solution of 2-chains as the solute and 1-chains as the solvent. As for usual solutions, such a solution exhibits a box-type spectrum H_{22} with the cut-off at τ_{22} and with its intensity P_{22} proportional to $w_2{}^{2}$. Similar to H_{11}, the H_{22} may be replaced by H_2. Thus, the portion of the spectrum in this range may be $w_2{}^{2}H_2(\tau/\lambda_{22})$.

Strictly speaking, the tube model does not predict a box-type spectrum but a wedge-type spectrum with its intensity being proportional to $\tau^{1/2}$ ($\tau < \tau_2$). However, it was found that many narrow distribution polymers usually exhibit a box-type spectrum with a considerably large intensity in the so-called rubbery plateau region ($\tau^* < \tau < \tau_2$). Thus for our blends also, the box-type spectrum H_{22} (representing the reptational modes of the 2-chains) may be extended down to τ_{11}. Thus, we may interpret that in the intermediate times $\tau_{11} < \tau < \tau_{12}$, not only the tube renewal process due to the reptation of 1-chains but also the reptation of the 2-chains from mixed type-1 and type-2 slip-links may be taking place simultaneously. This contribution may also be approximated by $w_2{}^{2}H_2$. The right-hand-side column of Figure 12 illustrates these situations.

By summing up all these contributions, we obtain a blending law valid for the blends with $w_2 > w_c$ as

$$H_B(\tau) = w_1H_{11}(\tau/\lambda_{11}) + w_2H_{12}{}^{b}(\tau) + f(w_2)H_{12}{}^{w}(\tau) + w_2{}^{2}H_{22}(\tau/\lambda_{22}) \simeq w_1H_1(\tau/\lambda_{11}) + w_2H_2(\tau)|_{\tau<\tau_{11}} + f(w_2)H_{12}{}^{w}(\tau) + w_2{}^{2}H_2(\tau/\lambda_{22})|_{\tau_{11}<\tau<\tau_{22}} \quad (13)$$

Here λ_{22} represents the shift between τ_{22} and τ_2 (cf. Figure 7). Again, the first two terms on the right-hand side of eq 13 are zero for $\tau > \tau_{11}$, while the third and fourth terms are effective in the ranges $\tau_{11} < \tau < \tau_{12}$ and $\tau_{11} < \tau < \tau_{22}$, respectively.

For the blends with $N_1 \ll N_2$, and hence $\tau_{11} \ll \tau_{12} \ll \tau_{22}$, the tube renewal process would not affect the terminal zone of the H_{22}. Then, if we employ the Doi theory incorporating contour length fluctuation eq 10, we have

$$\lambda_{22} = w_2{}^{1.4} \quad (14a)$$

On the hand, if we employ the original Dai–Edwards theory of pure reptation, we have[7]

$$\lambda_{22} = w_2 \quad (14b)$$

Although the difference between these λ_{22} is not large and indistinguishable in the range of w_2 (≥20 wt %) in question, the former appears to be more consistent with the experimental results obtained (e.g., eq 6).

The general behavior of the relaxation spectra shown in Figures 4–6 seems to be well described by our blending law. However, for the blends with $w_2 > w_c$, it is difficult to analyze the contribution of $H_{12}{}^{w}$ in the time scale $\tau_{11} < \tau < \tau_{12}$ from the raw H data alone. To do this, the relaxation spectra of the component 1- and 2-chains (given in a double-logarithmic scale) were first shifted horizontally by the amounts log (λ_{11}) and log ($\lambda_{22} = w_2{}^{1.4}$), and then, vertically by the amounts log w_1 and log $w_2{}^{2}$, respectively. The shifted spectra were subtracted from the observed one of the blend. Then we examined whether the considerable intensity remains at the intermediate time or not, and if it remains, we also examined the shape of the remaining spectrum. Figure 13 shows examples of such procedures applied to $H_B(\tau)$ at 143 °C of 20 and 40 wt % L407/L36 blends. We see that a considerably large spectrum $f(w_2)H_{12}{}^{w}$ remains and it looks like the Rouse-wedge with the characteristic time τ_{12} almost independent of w_2, as anticipated.

Since we could not determine the spectra for L1070 and L2580 samples, we employed an adequately shifted spectrum of L407 to analyze the data for the blends containing L1070 or L2580 samples. This approximation might introduce some ambiguities in the estimation of τ_{12} and P_{12} for the blends containing L1070 and L2580 (filled symbols in Figures 7 and 9). However, as can be seen in Figures 7 and 9, the general features of the w_2 dependence of τ_{12}

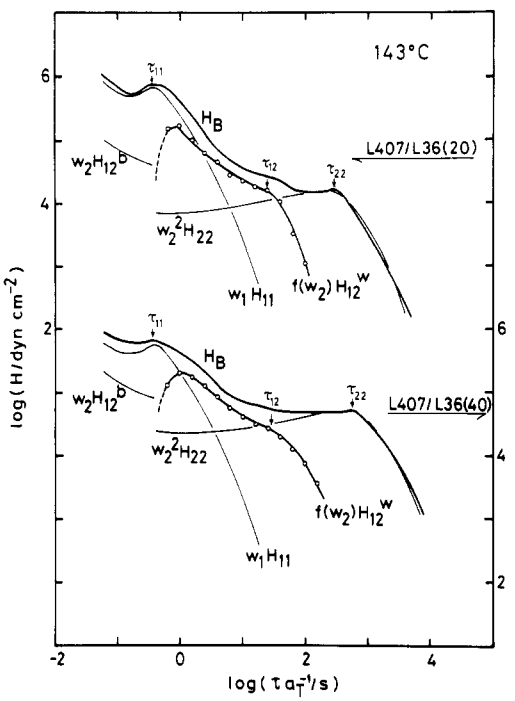

Figure 13. Examples of applying the blending law eq 13 for the relaxation spectra of 20 and 40 wt % L407/L36 blends at 143 °C.

and P_{12} for these blends agree with those for the L407 blends, for which both H_1 and H_2 were determined unambiguously from experiments. Thus we may conclude that the general features of τ_{12} and P_{12} are valid for all the blends examined.

Here we should probably comment on a blending law proposed by Masuda et al.,[25] because it is derived on the basis similar to ours. Masuda's law reads

$$H_B(\tau) = w_1H_1(\tau) + w_1w_2H_{12}(\tau) + w_2^2H_2(\tau/\lambda_{22}) \quad (15)$$

where H_{12} represents the contribution from the tube renewal process. Their H_{12} sometimes looks like box-type with the characteristic time τ_{12} proportional to $w_2^{1.5}M_{w1}^{3.5}M_{w2}^{1.5}$. Comparing eq 13 and 15, we notice that if we put $f(w_2) = w_1w_2$ and replace our H_{12}^w by their H_{12}, then both laws are *formally* identical in the time scale $\tau_{11} < \tau < \tau_{22}$. Their intensity factor w_1w_2 is qualitatively similar to our $f(w_2)$ except theirs has a maximum at $w_2 = 0.5$. We examined $f(w_2)$ only for those with $w_2 \leq 0.4$.

On the other hand, the w_2 dependence of τ_{12} and the shape of the H_{12} do not exactly match with our results. We speculate that this discrepancy may be attributed to the difference in the M_{w2}/M_{w1} ratio of the blends tested. Our blends have the ratio larger than 10, while their blends often have the much smaller ratio. Obviously, the molecular picture that a blend can be regarded as a concentrated solution of 2-chains at long times is valid only when $\tau_{22} \gg \tau_{12}$. If the M_{w2}/M_{w1} ratio is not large enough, the characteristic time τ_2 may not be very much longer than τ_{12}, or even the latter might exceed the former. Under such a situation the tube renewal and reptational modes of the 2-chain might not be separated. Then the portions ($H_{12}^b + H_{12}^w$ in our law and H_{12} in theirs) of the spectrum involving these mixed relaxation modes might take different forms.

Comparison with Experiments. A critical test of many previous blending laws[14-22] was made by comparing the molecular weight dependences of η_0 and J_e^0. Accordingly, we test our law with these quantities.

Zero-Shear Viscosity. Figure 14 shows plots of η_0 at 143 °C vs. the weight-average molecular weight $M_w = w_1M_{w1} + w_2M_{w2}$ of the blends in double-logarithmic scale. The filled symbols represent the data for narrow MWD polystyrenes. The data for the component polymers with high molecular weight and those for the blends with large w_2 ($\gg w_c$) obey the well-known 3.5th power law. However, when w_2 is small so that the M_w is not much different from M_{w1}, the η_0 data do not obey the 3.5th power law. This is not surprising because the L22 and L36 samples themselves have rather low molecular weights and their η_0 data do not exactly obey the 3.5th power law. However, a crucial point is that their viscosity cannot be reduced by the M_w alone.

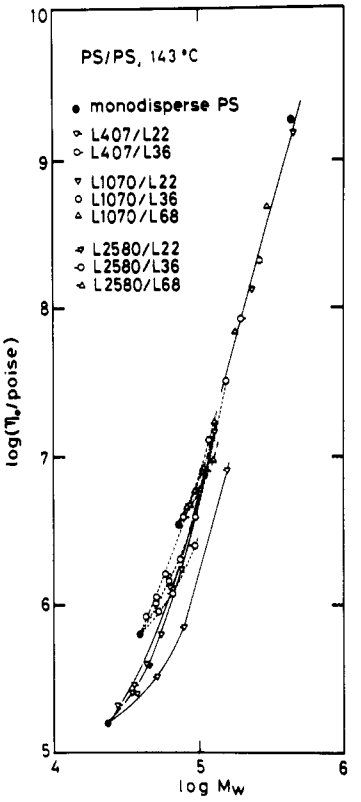

Figure 14. Dependence of the zero-shear viscosity η_0 at 143 °C on the weight-average molecular weight M_w of the blends. The filled symbols show η_0 for monodisperse PS samples.

Employing eq 12 for the relaxation spectrum of such dilute blends and neglecting the small difference between τ_1 and τ_{11}, we obtain

$$(\eta_0)_B = w_1(\eta_0)_1 + w_2[(\eta)_{12}^b + (\eta)_{12}^w] \quad (16)$$

where the quantities with B, 1, and 12 denote those derived from the corresponding portions of the spectrum. In some sense, eq 16 is a representation of a dilute solution viscosity of 2-chain in the solvent 1-chain. Figure 15 shows the plot of $(\eta_0)_B - w_1(\eta_0)_1$ vs. w_2 according to eq 16. For such dilute blends, the empirically determined quantity $(\eta_0)_B - w_1(\eta_0)_1$ is proportional to w_2, as anticipated from eq 16.

On the other hand, for concentrated blends with large w_2, we must employ eq 13 to calculate $(\eta_0)_B$, in which the contribution from the last term $w_2^2H_{22}(\tau/\lambda_{22}) \simeq w_2^2H_2(\tau/\lambda_{22})$ becomes dominant. Thus, eq 13 gives

$$(\eta_0)_B \simeq w_2^2\int_0^\infty H_2(\tau/\lambda_{22})\,d\tau = w_2^2\lambda_{22}\int_0^\infty H_2(\tau')\,d\tau' = w_2^{3.4}(\eta_0)_2 \propto (w_2M_{w2})^{3.4} \quad (17)$$

where eq 14a for λ_{22} is employed. For the blends with large w_2, the M_w is close to w_2M_{w2} and eq 17 agrees with the 3.5th power law. For example, $\log M_w - \log(w_2M_{w2}) < 0.05$ for the present blends with $w_2 \geq 40$ wt %. Our blending law

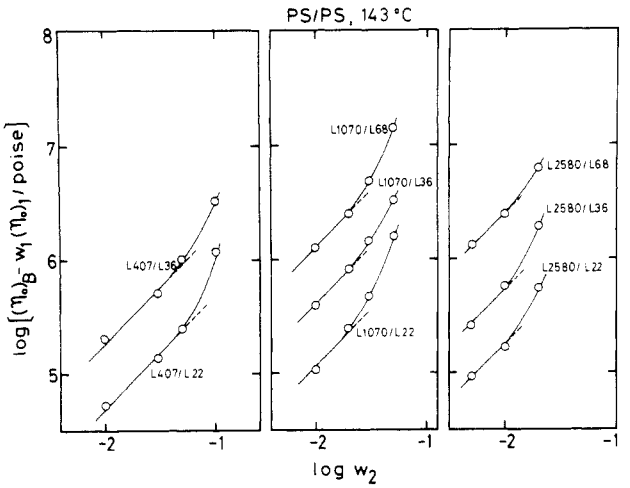

Figure 15. Plots of $(\eta_0)_B - w_1(\eta_0)_1$ of the binary blends at 143 °C against the content w_2 of the 2-chains.

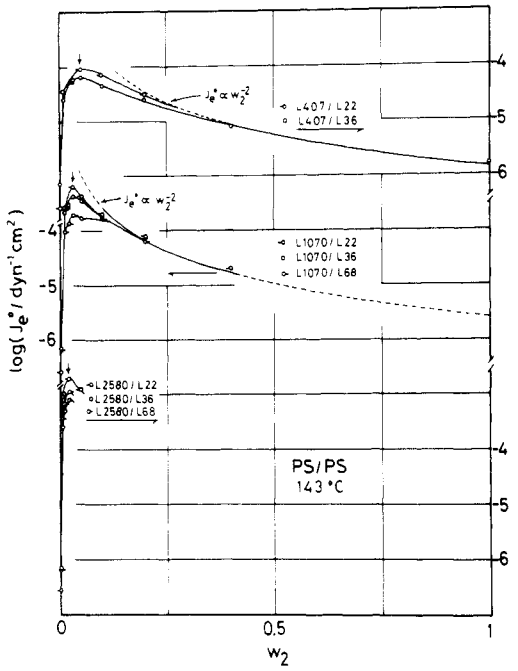

Figure 16. w_2 dependence of the steady-state recoverable compliance J_e^0 of the binary blends at 143 °C.

describes fairly well the $(\eta_0)_B$ of the blends.

Steady-State Recoverable Compliance. Figure 16 shows the w_2 dependence of J_e^0 at 143 °C of the blends. We see that for the blends with large w_2 the J_e^0 is proportional to w_2^{-2}, as already reported by many authors.[1,2,15-17] Besides these results, we notice that the J_e^0 vs. w_2 plots exhibit a sharp peak at about w_c, as indicated by the arrows.

For dilute blends with small $w_2 < w_c$, we obtain from eq 12

$$(J_e^0)_B(\eta_0)_B^2 = \int_0^\infty H_B(\tau)\tau\, d\tau = w_1(J_e^0)_1(\eta_0)_1^2 + w_2(J_e)_{12}^b[(\eta)_{12}^b]^2 + w_2(J_e)_{12}^w[(\eta)_{12}^w]^2 \quad (18)$$

where the small difference between τ_1 and τ_{11} is again neglected. Figure 17 shows the plot of the empirically determined quantity $(J_e^0)_B(\eta_0)_B^2 - w_1(J_e^0)_1(\eta_0)_1^2$ against w_2 according to eq 18. Again, the proportionality of this quantity and w_2 is satisfied in dilute blends.

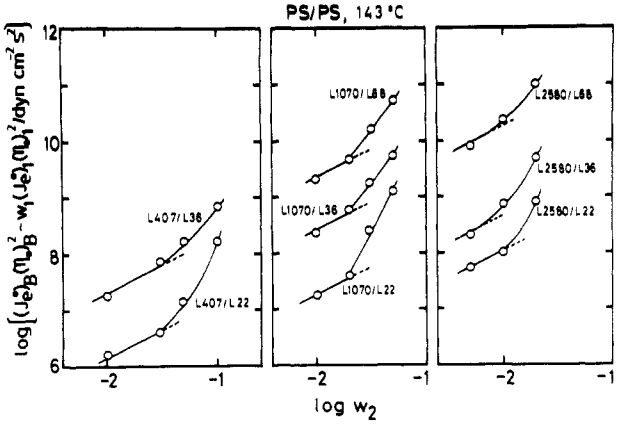

Figure 17. Plots of $(J_e^0)_B(\eta_0)_B^2 - w_1(J_e^0)_1(\eta_0)_1^2$ of the binary blends at 143 °C against the content w_2 of the 2-chains.

On the other hand, applying eq 13 for concentrated blends with large w_2, we have

$$(J_e^0)_B(\eta_0)_B^2 \cong w_2^2\int_0^\infty H_2(\tau/\lambda_{22})\tau\, d\tau = w_2^2\lambda_{22}^2\int_0^\infty H_2(\tau')\tau'\, d\tau' = w_2^{4.8}(J_e^0)_2(\eta_0)_2^2 \quad (19)$$

Then, from eq 17 and 19, we have

$$(J_e^0)_B = w_2^{-2}(J_e^0)_2 \quad (20)$$

Thus, eq 13 fairly well describes the behavior of $(J_e^0)_B$ at large w_2 as well. In this connection it should be noted that the sharp peak in $(J_e^0)_B$ appears to correspond to the crossover of the spectrum from that of eq 12 to that of eq 13.

All the results on the H_B, $(\eta_0)_B$, and $(J_e^0)_B$ appear to justify our blending law for the blends composed of two narrow distribution polymers having large molecular weight ratio.

Here, we should comment on the key parameters describing the viscoelastic properties of binary homopolymer blends. In many previous papers, the average molecular weights such as M_n, M_w, M_z, etc. were regarded as the key parameters for $(\eta_0)_B$ and $(J_e^0)_B$. However, as long as we incorporate the tube renewal process in the blending law, the key parameters should be $N_{e2}(w_2)$ and w_2 but not the average molecular weights.

Finally, we should also comment on the studies by the Berkeley group.[10,20,22] Although their picture is based on the extended Rouse model and differs much from ours, some results presented in this paper such as the w_2-independent τ_{11} and the proportionality between $(\eta_0)_B - w_1(\eta_0)_1$ and w_2 at small w_2 are also explained by their theory.

Acknowledgment. We thank Professor Toshiro Masuda and Dr. Masaoki Takahashi of the Department of Polymer Chemistry, Kyoto University for their valuable discussion with us. We thank Dr. Yoshiyuki Einaga of this department for his comments and criticism of our paper. We also thank Professor M. C. Williams, University of California, Berkeley, for his detailed and helpful criticism and comments. Some polystyrene samples used were supplied by Dr. Mitsutoshi Fukuda, Toyo Soda Mfg. Co., Ltd., whom we thank.

Registry No. Polystyrene (homopolymer), 9003-53-6.

References and Notes

(1) Ferry, J. D. "Viscoelastic Properties of Polymers", 3rd ed.; Wiley: New York, 1980.
(2) Graessley, W. W. *Adv. Polym. Sci.* **1974**, *16*.

(3) Bueche, F. *J. Chem. Phys.* **1956**, *25*, 599.
(4) Graessley, W. W. *J. Chem. Phys.* **1965**, *43*, 2696; **1967**, *47*, 1942; **1971**, *54*, 5143.
(5) de Gennes, P.-G. *J. Chem. Phys.* **1971**, *55*, 572.
(6) de Gennes, P.-G. "Scaling Concepts in Polymer Physics"; Cornell University Press: Ithaca, NY, 1979.
(7) Doi, M.; Edwards, S. F. *J. Chem. Soc., Faraday Trans. 2* **1978**, *74*, 1789; **1978**, *74*, 1802; **1978**, *74*, 1818; **1979**, *75*, 38.
(8) Doi, M. *J. Polym. Sci., Polym. Phys. Ed.* **1980**, *18*, 1005; **1980**, *18*, 1981.
(9) Evans, K. E.; Edwards, S. F. *J. Chem. Soc., Faraday Trans. 2* **1981**, *77*, 1891; **1981**, *77*, 1913; **1981**, *77*, 1929.
(10) Hansen, D. R.; Williams, M. C.; Shen, M. *Macromolecules* **1976**, *9*, 345. Hong, S. D.; Hansen, D. R.; Williams, M. C.; Shen, M. *J. Polym. Sci., Polym. Phys. Ed.* **1977**, *15*, 1869.
(11) Klein, J. *Macromolecules* **1978**, *11*, 852.
(12) Graessley, W. W. *Adv. Polym. Sci.* **1982**, *47*.
(13) Doi, M. *J. Polym. Sci., Polym. Phys. Ed.* **1983**, *21*, 667.
(14) Ninomiya, K. *J. Colloid Sci.* **1959**, *14*, 49. Ninomiya, K.; Ferry, J. D. *Ibid.* **1963**, *18*, 421.
(15) Masuda, T.; Kitagawa, K.; Inoue, T.; Onogi, S. *Macromolecules* **1970**, *2*, 116.
(16) Bogue, D. G.; Masuda, T.; Einaga, Y.; Onogi, S. *Polym. J.* **1970**, *1*, 563.
(17) Prest, W. M.; Porter, R. S. *Polym. J.* **1973**, *4*, 154. Prest, W. M. *Ibid.* **1973**, *4*, 163.
(18) Kurata, M.; Osaki, K.; Einaga, Y. *J. Polym. Sci., Polym. Phys. Ed.* **1974**, *12*, 849.
(19) Friedman, E. M.; Porter, R. S. *Trans. Soc. Rheol.* **1975**, *19*, 493.
(20) Soong, D. S.; Shen, M.; Hong, S. D. *J. Rheol.* **1979**, *23*, 301. Soong, D. S.; Shyu, S. S.; Shen, M.; Hong, S. D.; Moacanin, J. *J. Appl. Phys.* **1979**, *50*, 6007. Soong, D. S.; Shyu, S. S.; Shen, M. *J. Macromol. Sci., Phys.* **1981**, *B19*, 49.
(21) Kinouchi, M.; Takahashi, M.; Masuda, T.; Onogi, S. *J. Soc. Rheol. Jpn.* **1974**, *4*, 25.
(22) Liu, T. Y.; Soong, D. S., Williams, M. C. *J. Rheol.* **1983**, *27*, 7.
(23) Graessley, W. W. *J. Polym. Sci., Polym. Phys. Ed.* **1980**, *18*, 27.
(24) Kurata, M. *Macromolecules* **1984**, *17*, 895.
(25) Masuda, T.; Yoshimatsu, S.; Takahashi, M.; Onogi, S. *Polym. Prepr. Jpn.* **1983**, *32*(9), 2365.
(26) Markovitz, H. *J. Appl. Phys.* **1952**, *23*, 1070.
(27) Tschoegl, N. W. *Rheol. Acta* **1971**, *10*, 582.
(28) The observed M_{w1}^3 dependence (rather than $M_{w1}^{3.4}$) of τ_{12} (eq 5) implies that the tube renewal process is taking place essentially by the *pure* reptation of 1-chains without involving other mechanisms such as the contour length fluctuation, as suggested by Klein[11] and Graessley.[12] This is presumably because the tube renewal process is governed by the diffusion (not by the stress relaxation) of the tube forming 1-chains. In fact, observed molecular weight dependence of the (macroscopic) diffusion coefficient D_G ($\propto M^{-2}$)[29,30] was successfully accounted by the tube model incorporating only the *pure* reptation, while the $M^{3.4}$ dependence of η_0 was not. In other words, the mechanical relaxation of the 1-chain takes place by all the mechanisms releasing its constraints but its diffusion dominantly by reptation of the 1-chain.
(29) Klein, J. *Philos. Mag.* **1981**, *43*, 771.
(30) Leger, L.; Hervet, H.; Rondlez, F. *Macromolecules* **1981**, *14*, 1732.
(31) Osaki, K.; Nishizawa, K.; Kurata, M. *Macromolecules* **1982**, *15*, 1068.
(32) According to Doi,[13] $N^3N_e^{-1}[1 - 1.47(N_e/N)^{0.5}]^2$ is almost proportional to $N_e^{-1.4}N^{3.4}$ in the range $5 < N/N_e < 50$ and we obtain eq 10′ and 14a by putting $N_e \propto w_2^{-1}$.
(33) Strictly speaking, this replacement is only approximate because the cut-off time τ^* for the wedge spectrum in the transition zone for the 1-chain does not depend on w_2 while that τ_{11} for its box spectrum depends on w_2. However, the shift of τ_{11} is not large as shown in Figure 7, and we employ this approximation at present for simplicity.

Morphological and Viscoelastic Properties of Poly(styrene-*b*-butadiene-*b*-4-vinylpyridine) Three-Block Polymers of the ABC Type

Itaru Kudose and Tadao Kotaka*

Department of Macromolecular Science, Faculty of Science, Osaka University, Toyonaka, Osaka 560, Japan. *Received October 19, 1983*

ABSTRACT: A series of poly(styrene-*b*-butadiene-*b*-4-vinylpyridine) three-block (SBP) polymers of the ABC type, in which the composition was roughly *X*:1:1 with *X* varying from 1 to 8, were prepared. Their morphological and viscoelastic properties were compared with those of our previous samples having 1:*Y*:1 composition with *Y* varying from 1 to 4. The polymers were cast from $CHCl_3$ and from butyraldehyde (BA)/$CHCl_3$ (9/1 (v/v)) or tetrahydrofuran/methanol (4/1 or 9/1 (v/v)) mixtures (BA-system solvents). SBP samples having roughly 1:1:1 composition cast from $CHCl_3$ exhibited a "ball-in-a-box" structure, in which spherical poly(4-vinylpyridine) (P4VP) domains enclosed by polybutadiene (PB) shells were embedded in the polystyrene (PS) matrix phase. The size of the P4VP balls became progressively smaller with decreasing P4VP block length. The same samples with 1:1:1 composition cast from a BA-system solvent exhibited "three-layer-lamellar" morphology. With increasing *X*, the P4VP lamellae changed to cylinders and finally to spheres surrounded by PB shells, and the PS lamellae to the matrix. The specimens having P4VP spherical domains with PB shells exhibited only two viscoelastic relaxations corresponding to the glass transitions of the PB and PS phases. However, those having continuous P4VP (either lamellar or cylindrical) domains showed three transitions corresponding to the three phases. Probably, in the former, the mechanical excitations were absorbed and dissipated in the soft PB phase and not transmitted to the hard P4VP phase. However, in the latter, the P4VP phase forming continuous domains contributed to the mechanical loss.

Introduction

ABC three-block polymers[1-9] and their use as special function materials[1-3] have attracted much attention. Recently, work has been extended to explore three-component pentablock polymers of the BABCB type in search of more sophisticated applications.[10] In our previous publications,[6,7] we reported the synthesis, characterization, and morphological and mechanical properties of poly(styrene-*b*-butadiene-*b*-4-vinylpyridine) three-block polymers of the ABC type, which were referred to as SBP polymers. Although the morphology of microphase-separated structures in ABC three-block polymers[5-7] is in general more difficult to control than that in AB diblock copolymers,[11,12] we succeeded in developing two different types of unique morphology from an SBP polymer (coded as SBP-1 having approximately 1:1:1.3 volume composi-

0024-9297/84/2217-2325$01.50/0